# OCV Hysteresis Effect-based SOC Estimation in Extended Kalman Filter Algorithm for a $LiFePO_4$/C Cell

Jonghoon Kim, Gab-Su Seo, Changyoon Chun,
Bo-Hyung Cho
School of Electrical Engineering and Computer Science
Seoul National University, Seoul, Republic of Korea

Seongjun Lee
R&D Center
Samsung Techwin
Seongnam, Gyeonggi-Do, Republic of Korea

***Abstract*—This work investigates the electric characteristics of a carbon-coated $LiFePO_4$ cell with emphasis on their specific open-circuit voltage (OCV) characteristics, which include very flat OCV curves over the state-of-charge (SOC) and pronounced hysteresis phenomena. Examining discharging/ charging OCV measurement data of a $LiFePO_4$/C cell elucidates these phenomena. A simple equivalent circuit model is newly derived and used in an OCV hysteresis effect-based SOC estimation in the extended Kalman filter (EKF) algorithm. The interval of the relationship between the OCV and SOC is decreased to 5% ΔSOC steps to improve the performance of the algorithm. Additionally, to compensate the model errors caused by the equivalent circuit model and variation in parameters, a measurement noise model and data rejection are implemented because the model accuracy is critical in the EKF algorithm in order to obtain a good estimation. All SOC estimation results of the proposed work satisfy the specification within ±5%.**

***Keywords-state-of-charge(SOC);open-circuit voltage (OCV); extended Kalman filter (EKF); $LiFePO_4$/C .***

## I. INTRODUCTION

$LiFePO_4$/C (lithium iron phosphate/carbon-coated) based lithium ion battery has been considered as one of most promising candidates for large scale applications in the automotive and space industries because of its excellent chemical and thermal stability and low cost and long life, and its commercialization can offer wide applications especially to hybrid electric vehicles (HEVs) and plug-in HEVs (PHEVs).

A battery management system (BMS) is critical for maintain optimum battery performance, and the state-of-charge (SOC) is the most important factor controlled by such a system [1]-[3]. Precise SOC information is critical in practical applications, where it is necessary to determine how long the cell will last. This information is also used to know when to stop charging and discharging, as over-charging or over-discharging can cause permanent internal damage.

Accurate battery modeling is a key factor in battery system design process and operation. The open-circuit voltage (OCV) is considered as the representative factor for SOC estimation in BMS. The OCV characteristic for a $LiFePO_4$/C cell exhibit very flat OCV curves over the SOC range and pronounced hysteresis phenomena in comparison to the $LiCoO_2$ (lithium cobalt oxide) chemistry [4]-[6]. These unique OCV characteristics complicate the SOC estimation and can result in inaccurate battery information.

This work presents the SOC estimation in the extended Kalman filter (EKF) algorithm for a $LiFePO_4$/C cell. Important aspects characterizing the electrical behavior are outlined and adequate model approaches are presented, which enable the construction of the specific OCV characteristics. The flat OCV characteristic from the discharging/charging OCV measurement data are obtained. A simple equivalent circuit model considering the OCV hysteresis effect is derived to estimate SOC in the EKF. Additionally, the interval of each OCV-SOC relationship is modified to reduce the SOC estimation error, and a measurement noise model and data rejection are applied to compensate for the simplified battery modeling defects. When the proposed work is applied, all SOC estimates based on the EKF within ±5% of the values estimates by ampere-hour counting.

## II. OCV HYSTERESIS EFFECT FOR A $LiFePO_4$/C CELL

In the present work, a prismatic $LiFePO_4$/C cell with high capacity (14Ah) is explored to study cell's OCV hysteresis. The purpose of this section is to investigate how the OCV hysteresis effect influences SOC estimation. Fig. 1(a)-(b) displays two OCV curves at 0.5C rate in the discharging regime between 2.0V and 3.65V at 25°C. At each SOC steps, the cell is left in open circuit condition for 2 hours. The gradual discharging in both 5% and 10% ΔSOC steps was implemented. The OCV difference between SOC 0.7(70%) and 0.8(80%) are shown in Fig. 1(b). This OCV difference at same SOC range may result in poor BMS performance due to the SOC estimation that is based on OCV-SOC relationship in the EKF. Therefore, this work considers 5% ΔSOC steps for OCV measurement. In addition, the 5% ΔSOC steps emphasize the pronounced OCV hysteresis of the investigated cell. At the same SOC value, the OCV is higher after being charged than the OCV after being

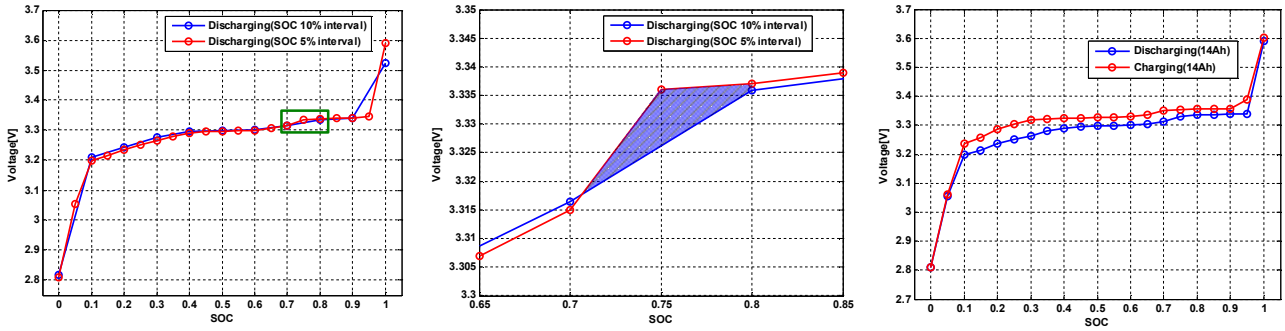


(a) (b) (c)

Figure 1. OCV hysteresis effect. (a) Discharging curves between 5% ΔSOC steps and 10% ΔSOC steps. (b) Enlarged OCV at SOC 0.7(70%)-0.8(80%). (c) Discharging/charging OCV curves in 5% ΔSOC steps.

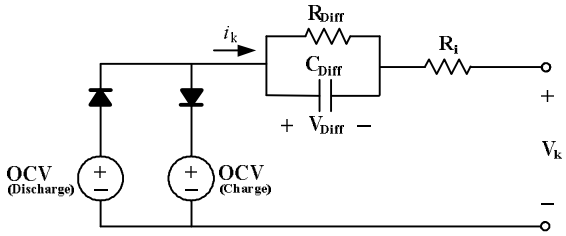


Figure 2. Simplified equivalent circuit model.

discharged, as illustrated in Fig. 1(c). The hysteresis effect is used to achieve and parameterize an appropriate battery equivalent circuit model that incorporates dynamic characteristic. Taking into above considerations into account, a simplified equivalent circuit model is developed, as shown in Fig. 2. It consists of two OCVs (SOC dependent), one for the charging and one for discharging selected by the current flow direction through two ideal diodes. There is also a series resistance $R_i$ connected in series to a parallel branch of a resistance $R_{Diff}$ and a capacitance $C_{Diff}$. This model is used for OCV hysteresis effect-based SOC estimation in the EKF algorithm.

## III. Extended Kalman Filter (EKF)

The extended Kalman filter (EKF) [7][8] is the optimum state estimator and is widely used. In general, the dynamic and measurement model used in the EKF are as follows:

$$x_k = f_{k-1}(x_{k-1}) + g(u_{k-1}) + w_{k-1} \qquad w_k \sim N(0, Q_k) \tag{1}$$

$$z_k = h_k(x_k) + i(u_k) + v_k \qquad v_k \sim N(0, R_k) \tag{2}$$

Here, $w_k$ represents the process noise and is assumed to be independent, zero-mean, Gaussian noise with a covariance matrix $Q_k$. The measurement noise $v_k$ is assumed to be independent, zero-mean, Gaussian noise with a covariance matrix $R_k$. Then, the equations that decide the Kalman gain $K_k$ are as follows:

$$K_k = P_k H_k^{\mathrm{T}} [H_k P_k H_k^{\mathrm{T}} + R_k]^{-1} \tag{3}$$

$$\hat{x}_k(+) = \hat{x}_k(-) + K_k[Z_k - H_k \hat{x}_k(-)] \tag{4}$$

where the error covariance matrix is $P_k$ and the measurement sensitivity matrix $H_k$.

SOC estimation requires an equivalent circuit model that represents the static and dynamic behavior of the battery. This can serve to construct the simplified model and prevent the EKF algorithm from measurement errors caused by inaccurate modeling. The simplified model (Fig. 2) has only two states. With the states incorporated, the dynamic model for the EKF is expressed as follows:

$$x_k = \begin{bmatrix} \mathrm{SOC}_{k+1} \\ \mathrm{V}_{\mathrm{Diff},k+1} \end{bmatrix} = \begin{bmatrix} 1 & 0 \\ 0 & 1 - \dfrac{\Delta t}{\mathrm{R}_{\mathrm{Diff}}\mathrm{C}_{\mathrm{Diff}}} \end{bmatrix} \begin{bmatrix} \mathrm{SOC}_k \\ \mathrm{V}_{\mathrm{Diff},k} \end{bmatrix} + \begin{bmatrix} -\dfrac{\Delta t}{\mathrm{C}_{\mathrm{n},k}} \\ \dfrac{\Delta t}{\mathrm{C}_{\mathrm{Diff}}} \end{bmatrix} i_k \tag{5}$$

The measurement model and the terminal voltage of the battery are expressed by a nonlinear function as follows:

$$\mathrm{V}_k = h_k(\mathrm{OCV}, \mathrm{V}_{\mathrm{Diff}}) - \mathrm{R}_i i_k = \mathrm{OCV} - \mathrm{V}_{\mathrm{Diff}} - \mathrm{R}_i i_k \tag{6}$$

The OCV in the measurement equation is implemented by the OCV-SOC relationship.

$$\frac{\partial h_k}{\partial x_k} = \begin{bmatrix} \dfrac{\partial h_{\mathrm{soc}}(\mathrm{SOC})}{\partial \mathrm{SOC}} & 0 \\ 0 & -1 \end{bmatrix} \qquad \mathrm{OCV} = h_{\mathrm{soc}}(\mathrm{SOC}),\ h_{\mathrm{soc}} = f_{\mathrm{ocv}}^{-1} \tag{7}$$

## IV. Measuremet Noise Model and Data Rejection

Model errors are the voltage errors between the measured battery voltage and the model output voltage. The model errors are caused by the model simplification and variations in the parameters of the model. The reduced order model includes the slow dynamics of the simplified equivalent circuit model, but excludes the fast dynamics that cause model errors and can lead to inaccurate estimation. To overcome this challenge, the measurement noise model and data rejection are necessary to compensate the model errors caused by the fast dynamics. The parameters of the simplified equivalent circuit model vary with the SOC, the discharge/charge current rate and other battery characteristics. In these cases, the measurement noise model should compensate the model errors. The measurement noise model and data rejection are implemented by modifying the measurement noise covariance, $R_k$. As expressed in (3), the $R_k$ is an important factor in deciding the Kalman filter gain of the EKF [7]. When $R_k$ is large, the estimate mainly depends on the process model. When $R_k$ is small, the estimate mainly depends on the measurement model. As expressed in (8) and (9), the Kalman gain is varied according to the value of $R_k$. Data rejection is achieved when $R_k$ is infinite. By adopting

the measurement noise model and data rejection, the Kalman filter becomes more robust to model simplification errors and variations in model parameters.

$$If\ R_k = \infty \quad K_k = P_k H_k^T [H_k P_k H_k^T + \infty]^{-1} = 0 \tag{8}$$

$$If\ R_k = 0 \quad K_k = P_k H_k^T [H_k P_k H_k^T]^{-1} = H_k^{-1} \tag{9}$$

The circuit model parameters vary with the SOC. In SOC region, there is little parameter change in the model resulting in a flat OCV curve. However, model parameters vary largely on either extreme of the SOC region, below 10% and above 95%, as shown in Fig. 1(a). The measurement noise covariance in the extreme SOC region should be adjusted to compensate the errors. The measurement noise model is implemented by modifying $R_k$ according to the SOC region. Due to the fast dynamic RC ladder in the equivalent circuit model, the measurement voltage at the initial response of the step current does not match the output voltage in the reduced order model. To compensate for this error, the $R_k$ should be determined separately according to whether or not the voltage of the RC ladder can be approximated by $V_{Diff}^{Final} \approx R_{Diff} I$ . When a large discharging or charging current is imposed, the measurement noise model is applied to avoid the increased voltage error. The large current denotes a reference set current of 15A (1C), while the gain is defined as 5. During a current step, the RC ladder dynamics cause a model error that exists for a short period. The decision to accept or reject the data depends on the current step magnitude. If $\Delta I$ per sample time is larger than a set value, it is regarded as the step current and the data rejection is carried out. Three measurement noise models and data rejection are listed in Table I.

TABLE I. THREE MEASUREMENT NOISE MODELS AND DATA REJECTION IN THE EKF

| **Measurement noise model by SOCs** |
|---|
| $R_{k+1} = R_k$ for $(0.1 < SOC < 0.95)$ |
| $R_{k+1} = R_k \{1 + G_{SOC\_low}(0.1 - SOC)\}$ for extreme SOC $(SOC < 0.1)$ |
| $R_{k+1} = R_k \{1 + G_{SOC\_high}(SOC - 0.95)\}$ for extreme SOC $(SOC > 0.95)$ |
| $G_{SOC\_low} = G_{SOC\_high} = 15$ |
| **Measurement noise model by dynamics of diffusion** |
| $V_{Diff}^{Final} = R_{Diff} I \left(1 - e^{-\frac{t}{R_{Diff} C_{Diff}}}\right) + V_{Diff}^{Initial} \left(e^{-\frac{t}{R_{Diff} C_{Diff}}}\right)$ |
| $V_{Diff}^{Final} \approx R_{Diff} I$ (Fast dynamic) $\quad V_t = OCV - R_i I - V_{Diff}^{Final}$ |
| $R_{k+1} = R_k \{1 + G_{step}(step\_time)\}$ |
| $step\_time = 5$ |
| **Measurement noise model by battery current** |
| $R_{k+1} = R_k$ for reliable current $(\lvert i \rvert < 15A)$ |
| $R_{k+1} = R_k \{1 + G_i(\lvert i \rvert - 15A)\}$ for unreliable current $(\lvert i \rvert > 15A)$ |
| $G_i = 5$ |
| **Data rejection caused by the fast dynamic of the RC ladder** |
| $R_k = \infty$ for reject_time $(\Delta I > 15A)$ |
| $reject\_time = 100ms$ |

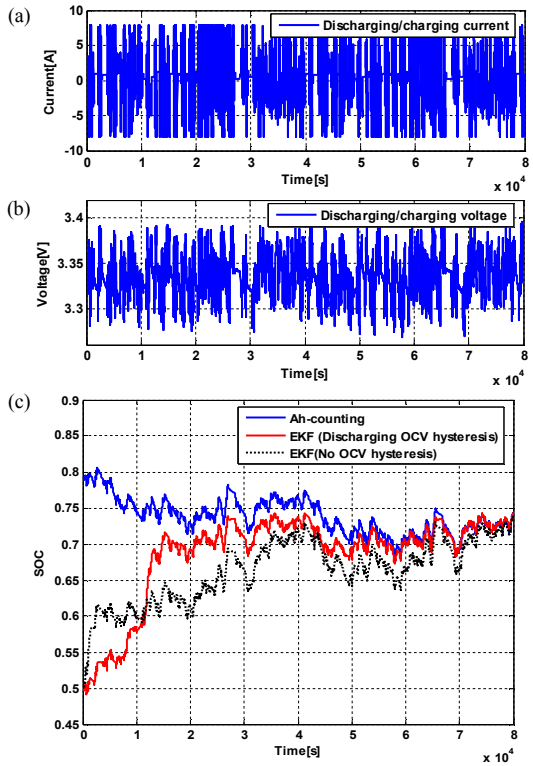


Figure 3. SOC estimation results. (a) Discharging/charging current profile (-8A~8A). (b) Discharging/charging voltage. (c) SOC estimation results of the two EKFs (Discharging OCV hysteresis, No OCV hysteresis) in comparison with ampere-hour counting (EKF initial SOC 0.5)

## V. VERIFICATION

The model parameters based on the voltage response are used to estimate the SOC ($R_i$=0.002095Ω, $R_{Diff}$=0.005361Ω, $C_{Diff}$=19399F). Fig. 4 shows the SOC estimation results of the two EKFs that take into account the discharging OCV hysteresis. Compared to SOC estimation that does not account for OCV hysteresis, the proposed SOC estimation technique is more accurate. As previously mentioned, the 5% ΔSOC steps and measurement noise model enables an improvement in the SOC estimation performance. The SOC difference between 5% ΔSOC steps and 10% ΔSOC steps is shown in Fig. 4(a)-(b). As shown in Fig. 4(c), the proposed SOC estimation approach satisfies the specification within ±5%. As shown in Fig. 4(d), measurement noise model is able to reduce the SOC estimation model error. Fig. 5 shows another SOC estimation results based on discharging/charging OCV hysteresis in 5% ΔSOC steps and measurement noise model.

## VI. CONCLUSION

This work deals with a SOC estimation of a $LiFePO_4$/C cell that includes flat OCV curves over the SOC. Incorporating discharging/charging OCV hysteresis, 5% ΔSOC steps, and a measurement noise model enables an improvement in the SOC estimation performance compared to the conventional method.

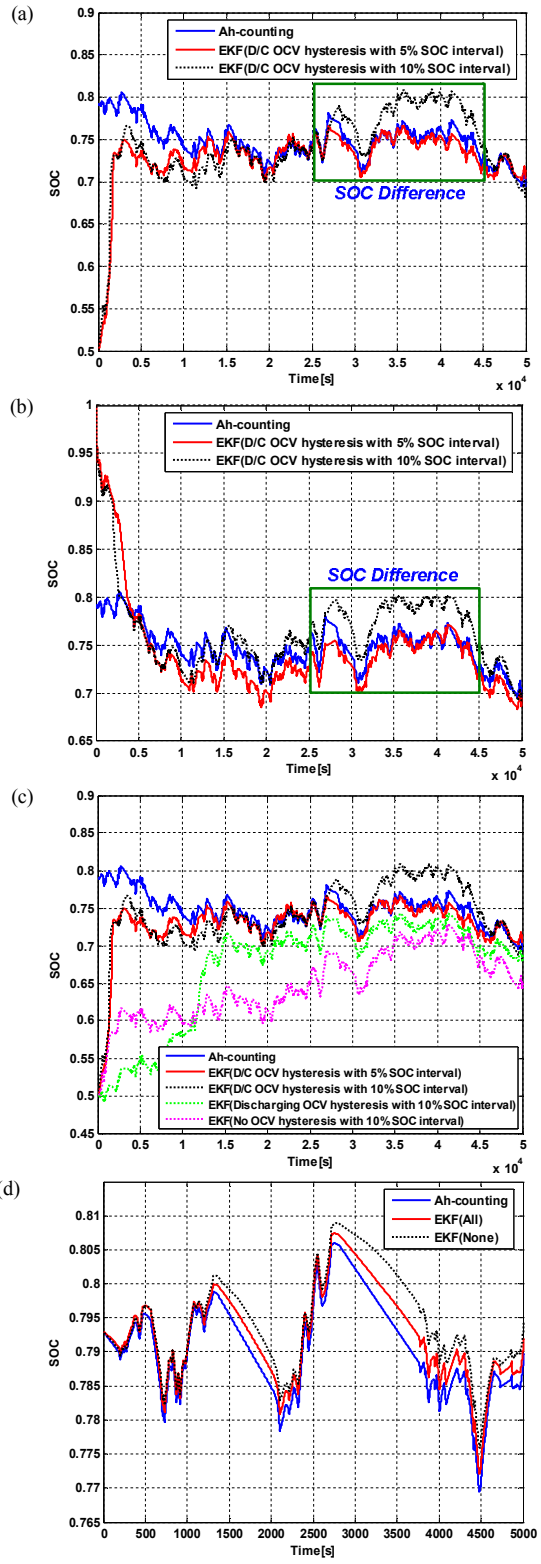


Figure 4. SOC estimation results based on discharging/charging OCV hysteresis between 5% ΔSOC steps and 10% ΔSOC steps. (a) EKF initial SOC 0.5. (b) EKF initial SOC 1. (c) SOC estimation result of the proposed work in comparision with the conventional method. (d) Measurement noise model by dyanmics of diffusion. **(Current profile -8A~8A)**

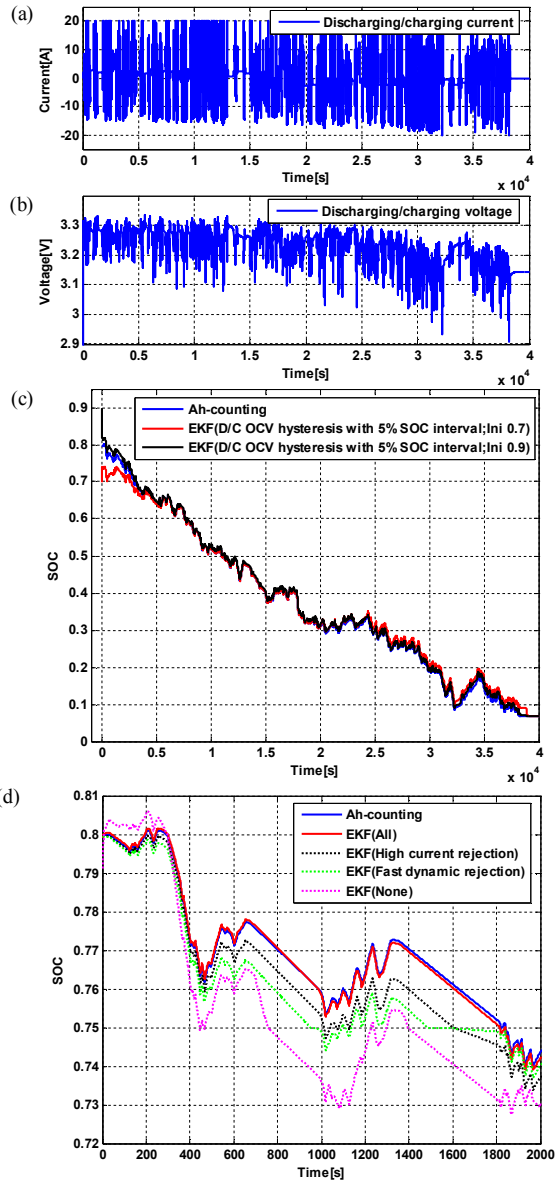


Figure 5. SOC estimation results. (a) Discharging/charging current profile (-20A~20A). (b) Discharging/charging voltage. (c) SOC estimation result of the proposed work in comparision with the conventional method (EKF initial SOC 0.7, 0.9) (d) Measurement noise model by battery current and dyanmics of diffusion.

## ACKNOWLEDGMENT

This research was conducted under the industrial infrastructure program for fundamental technologies which is funded by the Ministry of Knowledge Economy (MKE, Korea) and was supported by the New and Renewable Energy Program of the Korea Institute of Energy Technology Evaluation and Planning (KETETP) grant funded by the Korea government Ministry of Knowledge Economy (No. 20104010100490).

## REFERENCES


[1] M. Dubarry, N. Vuillaume, and B. Y. Liaw, "From single-cell model to battery pack simulation for Li-Ion batteries," *J. Power Sources*, vol. 186, pp. 500-507, Jan. 2009.

[2] V. Agarwal, K. Uthaichana, R. A. DeCarlo, and L. H. Tsoukalas, "Development and validation of a battery model useful for discharging and charging power control and lifetime estimation," *IEEE Trans. Energy Convers.*, vol. 25, no. 3, pp. 821-835, Sep. 2010.

[3] L. Maharjan, S. Inoue, H. Akagi, and J. Asakura, "State-of-charge (SOC)-balancing control of a battery energy storage system based on a cascade PWM converter," *IEEE Trans. Power Electron*., vol. 24, no. 6, pp. 1628-1636, Jun. 2009.

[4] A. Awarke, S. Lauer, S. Pischinger, and M. Wittler, "Percolation-tunneling modeling for the study of the electric conductivity in $LiFePO_4$ based Li-ion battery cathodes," *J. Power Sources*, vol. 196, pp. 405-411, Feb. 2011.

[5] Y. Zhang, C.-Y. Wang, and X. Tang, "Cycling degradation of an automotive $LiFePO_4$ lithium-ion battery," *J. Power Sources*, vol. 196, pp. 1513-1520, Feb. 2011.

[6] M. A. Roscher, J. Assfalg, and O. S. Bohlen, "Detection of Utilizable Capacity Deterioration in Battery Systems," *IEEE Trans. Veh. Technol.*, vol. 60, no. 1, pp. 98-103, Jan. 2011.

[7] G. L. Plett, "Extended Kalman filtering for battery management systems of LiPB-based HEV battery packs: Part 1-3," *J. Power Sources*, vol. 134, pp. 252-292, Aug. 2004.

[8] J. Kim and B. H. Cho, "State-of-Charge Estimation and State-of-Health Prediction of a Li-Ion Degraded Battery Based on an EKF Combined With a Per-Unit System," *IEEE Trans. Veh. Technol.*, vol. 60, no. 9, pp. 4249-4260, Nov. 2011.